Supporting Information

One-pot synthesis of photonic microparticles doped with light-emitting quantum dots

Simone Bertucci,[a,b] Davide Piccinotti,[a] Mauro Garbarino,[a] Andrea Escher,[b] Gianluca Bravetti,[c] Christoph Weder,[c,d] Paola Lova,[b] Davide Comoretto,[b] Ullrich Steiner,[c,d], Francesco Di Stasio,[a] Andrea Dodero,*[b,c,d]*

[a] Photonic Nanomaterials, Istituto Italiano di Tecnologia, Via Morego 30, 16163 Genoa, Italy
E-mail: francesco.distasio@iit.it

[b] Department of Chemistry and Industrial Chemistry, University of Genoa, Via Dodecaneso 31, 16146, Genoa, Italy

[c] Adolphe Merkle Institute, University of Fribourg, Chemin des Verdiers 4, 1700, Fribourg, Switzerland
E-mail: andrea.dodero@unifr.ch

[d] National Center of Competence in Research Bio-Inspired Materials, Chemin des Verdiers 4, 1700, Fribourg, Switzerland

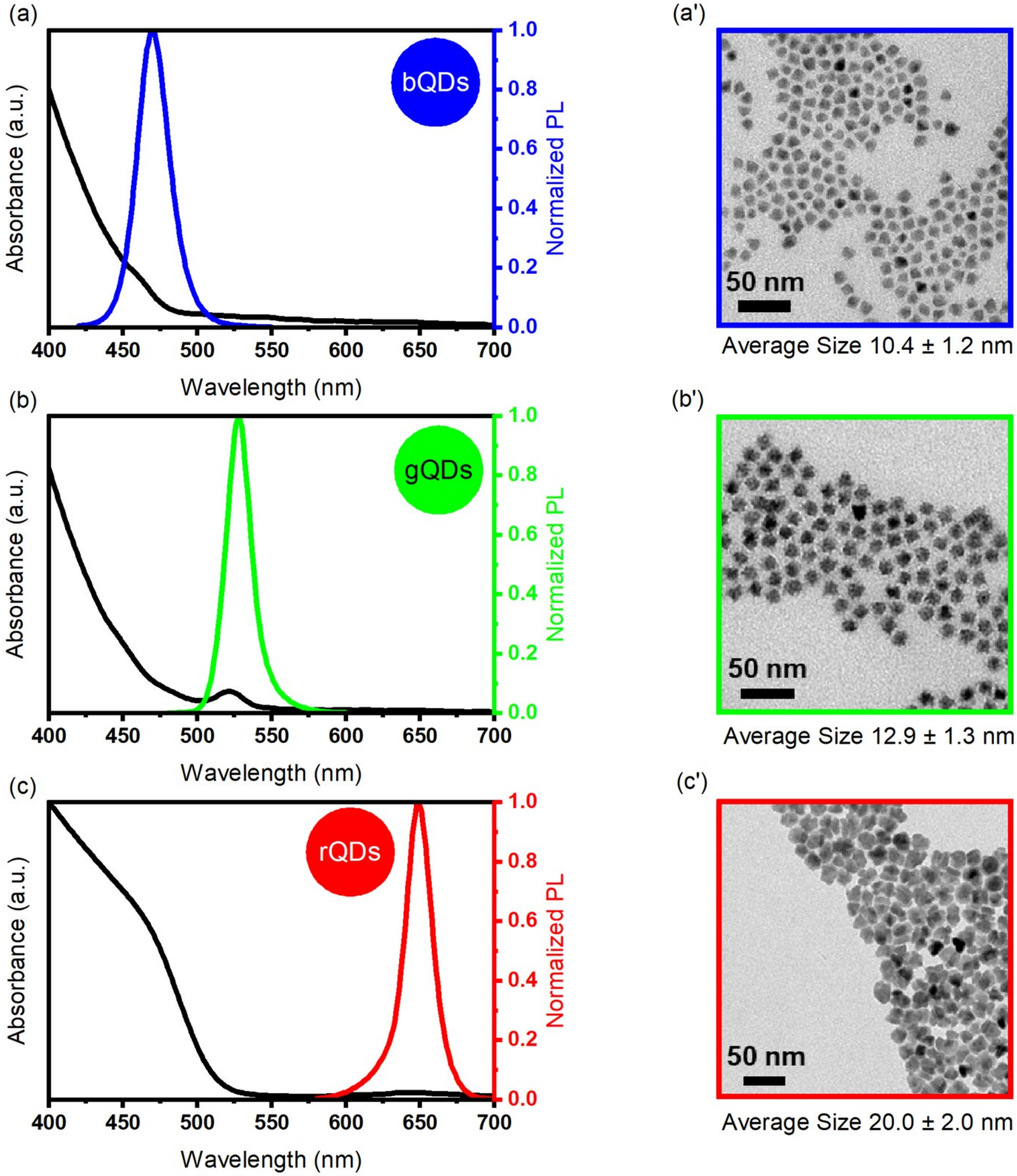

Figure S1. (a-c) Absorbance (black lines) and photoluminescence (colored lines) spectra, (a’-c’) TEM micrographs with relative average QDs size for blue (a, a’; bQDs), green (b, b’; gQDs), and red (c, c’; rQDs) quantum dots.

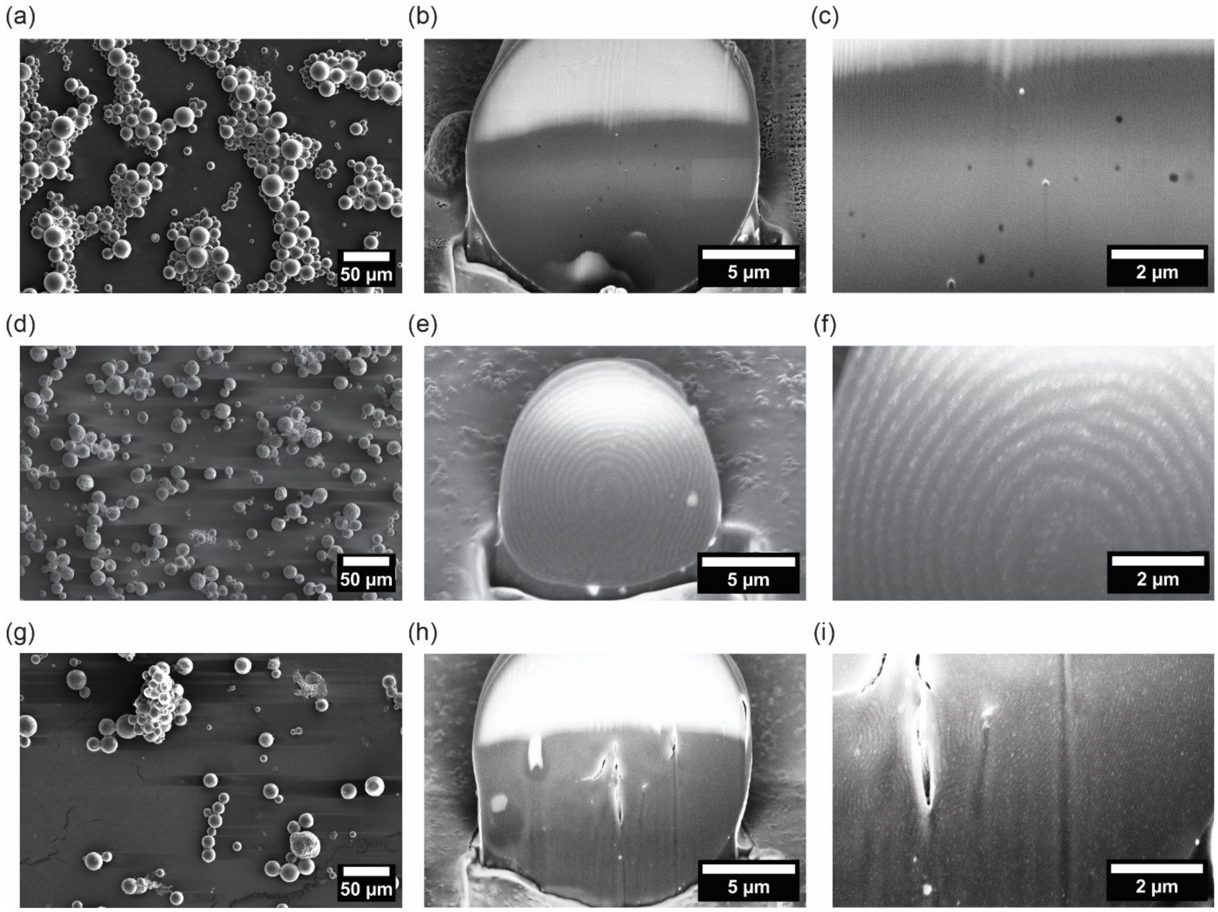

Figure S2. (a) Top view and (b-c) cross-section FIB-SEM micrographs of PS-PMMA reference microparticles, where the presence of embedded QDs cannot be confirmed. (d) Top view and (e-f) cross-section of PS-P2VP reference particles, where the loading of QDs into a specific polymer domain is evident. (g) Top view and (h-i) cross-section of P2VP-PMMA reference particles, where the loading of QDs into a specific polymer domain is evident despite the limited contrast between the polymer phases.

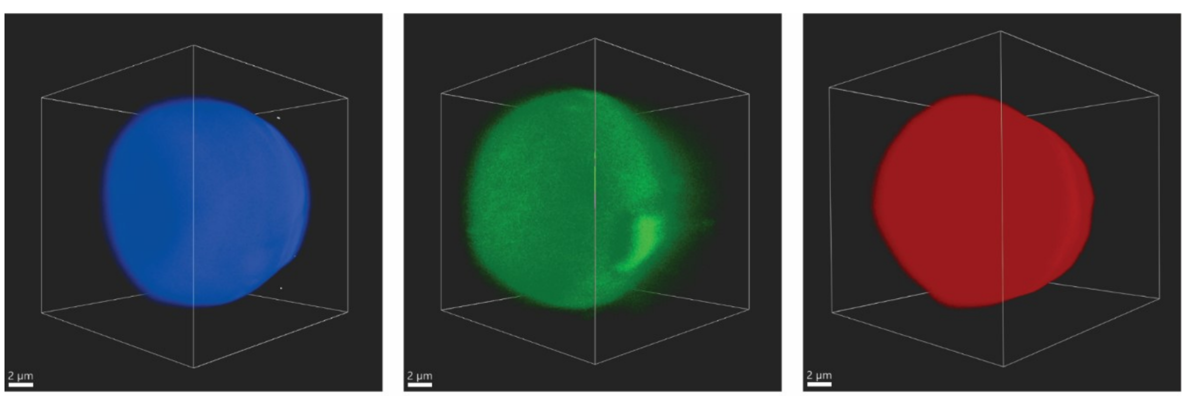

Figure S3. CLSM images of PS-P2VP microparticles containing blue, green, and red quantum dots. A consistent PL signal is detected within the entire volume of the particles, indicating a homogeneous distribution of the nanocrystals within the concentric lamellar structure.

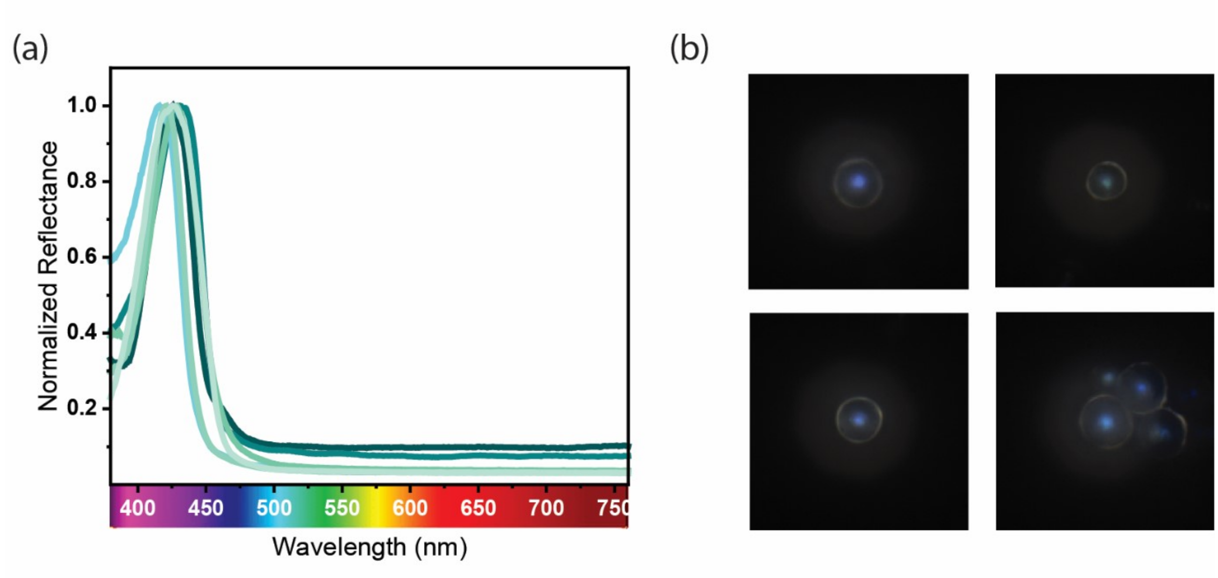

Figure S4. (a) Normalized reflectance spectra and (b) optical microscopy images of neat PS-P2VP BCP microparticles where small variations in the PBG position and particle size are detectable.

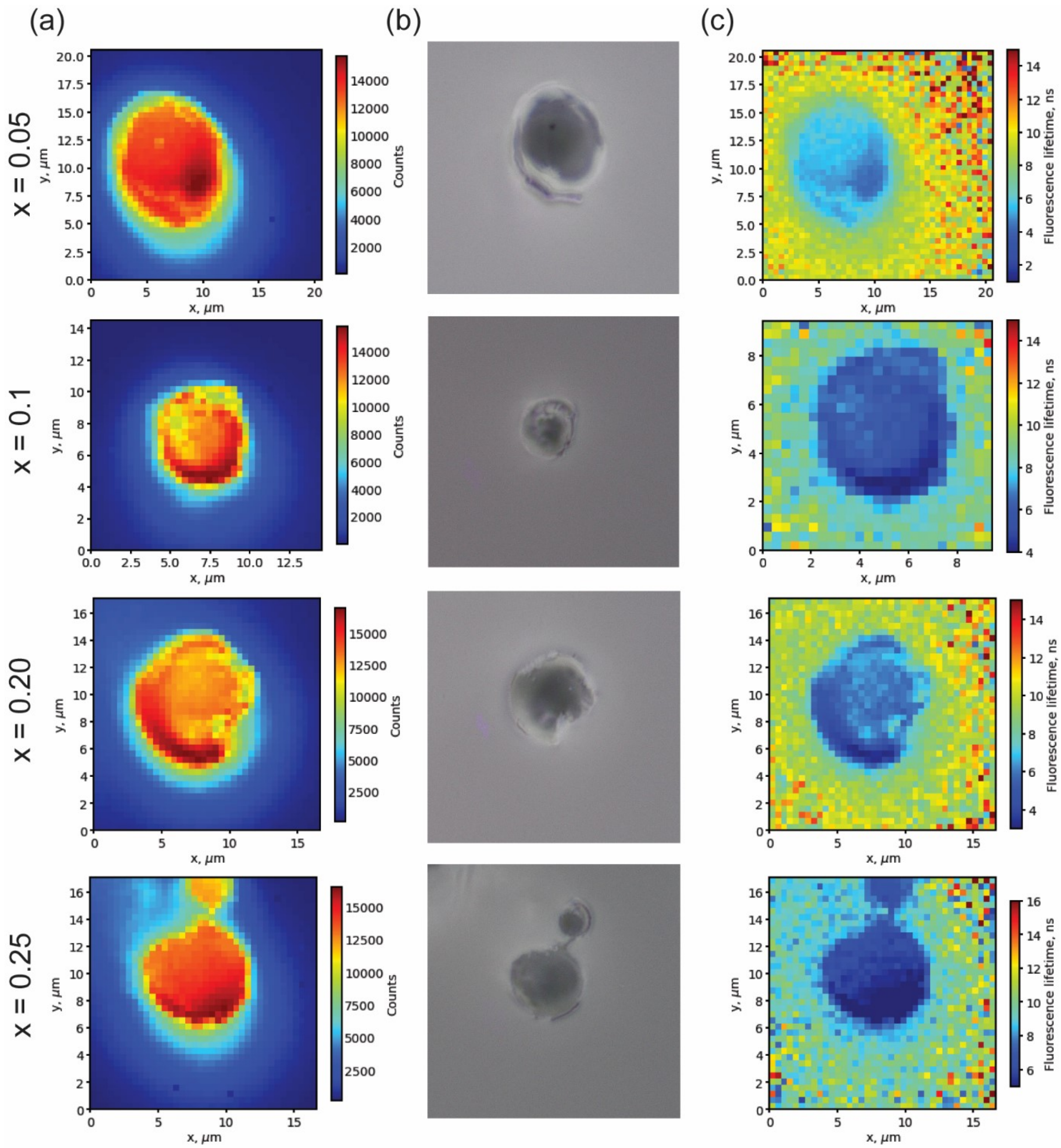

Figure S5. (a) 2D photoluminescence mapping, (b) optical microscopy images, and (c) lifetime mapping of PS-P2VP BCP(bQDs) microparticles with different *x*-ratios. All samples display a lower PL intensity at the particle edges, while no significant variations are depicted in terms of lifetime decay.

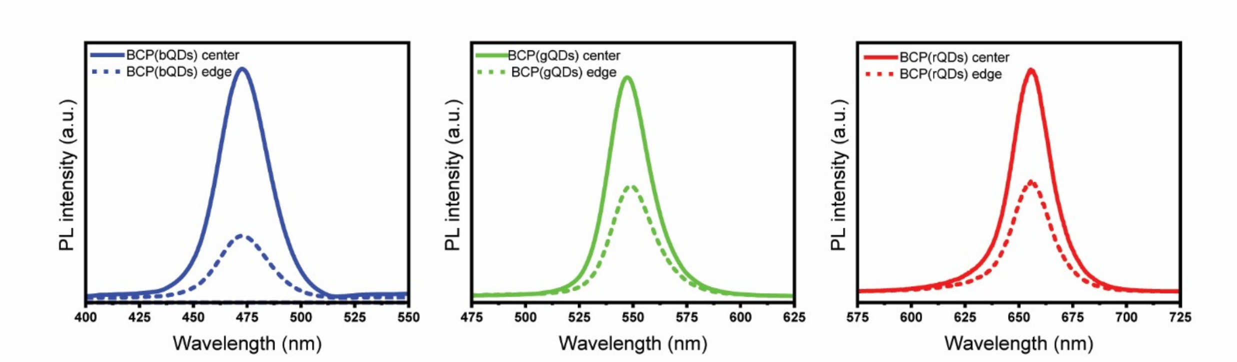

Figure S6. Comparison of the PL spectra measured on single PS-P2VP BCP(QDs) microparticles in their center (continuous line) and at their edge (dotted line). A marked decrease in the PL intensity is observable when compared to the signal at the center with that at the edge due to the lower number of excited quantum dots.

Table S1. Comparison of the measured and calculated λ_{max} values for pristine and hybrid photonic microparticles. Calculated values were obtained via the Bragg-Snell law using $n_{P2VP} = 1.62$ and $n_{PS} = 1.59$, with *d* retrieved from FIB-SEM micrographs. The discrepancy between the calculated (lower) and measured (higher) values quantitatively confirm the increse in the refractive index of P2VP domains upon the addition of the quantum dots.

Sample	d_{P2VP} (nm)	d_{PS} (nm)	λ_{max} – Measured (nm)	λ_{max} – Calculated (nm)
PS-P2VP	67.9	60.0	419	411
BCP(bQDs)	69.1	60.6	426	417
BCP(gQDs)	73.6	59.3	442	427
BCP(rQDs)	78.6	60.4	471	447

Fitting algorithm and parameters for TRPL measurements

The number of photons accounting for the decay of the exciton in the CdSe/CdS QDs is modeled as:

$$y = y_0 + A_1 e^{-t/\tau_1} + A_2 e^{-t/\tau_2}$$

where y is the number of photons measured, y_0 accounts for the background noise, and A_i and τ_i describe the amplitude and the decay time for each decay process. Retrieved values are shown in the table attached to Figure 3, while the fitting parameters are reported in Table S2 below. Mean values are calculated based on their relative weights.

Table S2. Fitting parameters for the calculation of PL lifetime decays ($\tilde{\tau}$) that are reported in Figure 3.

Sample	y_0	δy_0	A_1	δA_1	A_2	δA_2	τ_1 (ns)	$\delta\tau_1$	τ_2 (ns)	$\delta\tau_2$	R^2
bQDs	0.002	0.0003	0.759	0.005	0.231	0.005	11.98	0.289	22.67	1.48	0.999
BCP(bQDs)	0.003	0.0001	0.653	0.004	0.334	0.004	2.93	0.021	9.25	0.068	0.998
gQDs	0.005	0.0005	0.846	0.002	0.157	0.008	11.59	0.101	39.63	1.58	0.999
BCP(gQDs)	0.001	0.0011	0.736	0.004	0.230	0.003	1.10	0.013	9.58	0.013	0.997
rQDs	0.02	0.001	0.236	0.003	0.646	0.003	10.35	0.16	40.19	0.13	0.998
BCP(rQDs)	0.009	0.002	0.364	0.004	0.532	0.003	3.70	0.007	28.74	0.014	0.999

Table S3. Fitting parameters for the calculation of PL lifetime decays **($\tilde{\tau}$)** that are reported in Figure 5.

Sample	y_0	δy_0	A_1	δA_1	A_2	δA_2	τ_1 (ns)	$\delta\tau_1$	τ_2 (ns)	$\delta\tau_2$	R^2
x = 0.00	0.003	0.0001	0.653	0.004	0.334	0.004	2.93	0.021	9.25	0.068	0.998
x = 0.05	0.004	0.0002	0.491	0.009	0.352	0.010	2.87	0.053	9.61	0.153	0.999
x = 0.10	0.004	0.0002	0.613	0.013	0.327	0.014	3.53	0.004	10.51	0.232	0.999
x = 0.15	0.004	0.0002	0.474	0.008	0.406	0.009	2.79	0.005	9.82	0.129	0.999
x = 0.20	0.002	0.0001	0.430	0.010	0.371	0.005	3.25	0.008	10.97	0.09	0.973
x = 0.25	0.004	0.0002	0.501	0.010	0.338	0.010	3.13	0.059	10.09	0.176	0.991